Cell Tissue Res
DOI 10.1007/s00441-007-0382-x

REGULAR ARTICLE

Elevated expression of genes assigned to NF-κB and apoptotic pathways in human periodontal ligament fibroblasts following mechanical stretch

Nina Ritter · Eva Mussig · Thorsten Steinberg · Annette Kohl · Gerda Komposch · Pascal Tomakidi

Received: 22 November 2006 / Accepted: 15 January 2007

Abstract There is growing evidence that apoptosis involves the nuclear transcription factor NF-κB in conjunction with related genes. However, in the context of mechanical orthodontic forces, force-sensing target genes assigned to pathways of NF-κB and apoptosis have not been fully characterised. To contribute to the identification of putative target genes, we used cDNA arrays specific for NF-κB and apoptotic pathways and analysed elevated gene expression in primary human periodontal ligament fibroblasts (PDL-F) after a 6 h application of mechanical force. Among several identified genes (including several caspases), interleukin-1β (IL-1β) and NF-κB displayed significantly higher expression on the NF-κB array, whereas higher expression was obtained for BCL2-antagonist of cell death (BAD), member 6 of the TNF-receptor superfamily (FAS) and CASP2 and RIPK1 domain-containing adaptor with death domain (CRADD) on the apoptosis array. Based on a defined cut-off level of a more than 1.5-fold higher expression, this significance in elevated gene expression was corroborated by reverse transcription/polymerase chain reaction (RT-PCR). Here, semi-quantitative (sq) PCR revealed a more pronounced elevation of mRNA gene expression in PDL-F after 6 h of stretch, when compared with 12 h. Moreover, the elevation after 6 h as observed by sq-PCR was convergent with quantitative PCR (q-PCR). q-PCR yielded levels of 5.8-fold higher relative gene expression for IL-1β and 1.7-fold for NF-κB, whereas that computed for BAD indicated a 5.2-fold, for CRADD a 2.1-fold and for FAS a 2.0-fold higher expression. The data obtained from the expression analysis thus indicate a stretch-induced transcriptional elevation of genes assigned to the NF-κB and apoptotic pathways. This elevation may render them target candidates for being addressed by mechanical orthodontic forces.

Keywords Periodontal ligament · Periodontal ligament fibroblasts · Mechanical stretch · Apoptosis · cDNA microarray · Human

Introduction

In orthodontics, mechanical forces are used to induce orthodontic tooth movement, which is governed by remodelling changes in paradental tissues. Studies published so far have revealed extensive cellular activities in the periodontal ligament (PDL), involving fibroblasts, endothelial cells, osteoblasts, osteocytes and endosteal cells. In this context, mechanical stresses have been described as altering the structural properties of tissues at the cellular, molecular and genetic levels. Basically, the effects of mechanotherapy can be divided into rapid tissue reactions at the initial stage followed by later-occurring slower adaptive changes. In particular, force-induced tissue strain produces local alterations in vascularity and cellular and extracellular matrix

Nina Ritter and Eva Mussig contributed equally to the manuscript.

This work was supported by grants from the German Orthodontic Society/DGKFO to Eva Mussig (Science fund project no. 32, 2005) and from the DFG to Pascal Tomakidi (P.T. TO 195/6-1).

This article is dedicated to Professor Dr. Gerda Komposch due to her leadership of the Orthodontics Department for 28 years.

N. Ritter · E. Mussig · T. Steinberg · A. Kohl · G. Komposch · P. Tomakidi (✉)
Department of Orthodontics and Dentofacial Orthopaedics,
Dental School, University of Heidelberg,
Im Neuenheimer Feld 400,
69120 Heidelberg, Germany
e-mail: Pascal.Tomakidi@med.uni-heidelberg.de

(ECM) reorganisation (Waddington and Embery 2001). These alterations in turn lead to the synthesis and release of, for example, growth factors and mediators associated with inflammation (for a review, see Krishnan and Davidovitch 2006).

On the cellular level, force transmission implies changes in gene expression with respect to a broad spectrum of molecules, which in turn facilitate tooth movement (Meikle 2006). Examples of molecules shown to exhibit transcriptional and post-transcriptional changes in vitro and in vivo include integrins (Bolcato-Bellemin et al. 2000), ECM molecules (Sato et al. 2002; Redlich et al. 2004), proteases and TIMPs, which orchestrate ECM turn-over (Redlich et al. 2004; Ingman et al. 2005). Moreover, molecules associated with the differentiation of cells of mineralised tissues (Pavlin et al. 2001; Chiba and Mitani 2004) and mechanotransduction (Molina et al. 2001) are altered. Although limited in number, recent studies support evidence that apoptosis also occurs during orthodontic tooth movement (Rana et al. 2001; Hamaya et al. 2002), and that, in osteocytes, caspase-8 (CASP8) acts as a key executioner (Goga et al. 2006). In addition, the molecular regulation of tooth movement is also governed by the synthesis of inflammatory molecules. Results obtained in humans and animals indicate elevated levels not only for IL-1β and prostaglandin E2 (Lee et al. 2004; Yamaguchi et al. 2006), but also for tumour necrosis factor-α (TNF-α; Jager et al. 2005) and IL-8 (Tuncer et al. 2005).

Like IL-1β, TNF-α plays an important role in mediating immune and inflammatory responses. Moreover, it takes a significant part in the control of proliferation, differentiation and apoptosis, although it is a weaker inducer of extrinsic apoptosis compared with the TNF-related apoptosis-inducing ligand (TRAIL) and CD95 ligand (Baud and Karin 2001). Concerning cells of the periodontal tissues, TNF-α has currently been shown to trigger apoptosis in osteoblasts and PDL cells (Thammasitboon et al. 2006). Upon binding of TNF-α to its receptor TNF-R1, receptor clustering triggers one of two different pathways: a pro- or anti-apoptotic pathway (Liu et al. 1996). Both pathways coexist in a specific balance, each being promoted depending on the physiological conditions. Either the recruitment of the FAS-ligand-associated death domain (FADD) leads to the induction of apoptosis or the recruitment of the so-called TNF-receptor-associated factor (TRAF) proteins results in the activation of the transcription factor NF-κB (nuclear factor kappa B), which is commonly known to mediate cell survival pathways (Hsu et al. 1995; Krappmann et al. 1996). In addition to its important role in controlling immune function, cell proliferation and differentiation, NF-κB has so far been mainly described as inducing the expression of anti-apoptotic genes (Wang et al. 1998). One mechanism by which NF-κB exerts its function in an anti-apoptotic fashion is the activation of genes encoding for inhibitors of apoptosis proteins (c-IAPs). These c-IAPs interfere with the activation of effector CASPs (Wang et al. 1998). In this context, a potent inducer of NF-κB is the above-mentioned pro-inflammatory cytokine IL-1β. Whereas the IL-1β-mediated up-regulation of NF-κB has been described to reduce TRAIL-induced apoptosis in transformed keratinocytes, recent studies have reported that IL-1β is capable of significantly enhancing UV-B-mediated apoptosis in an NF-κB-dependent manner. This promotion of pro-apoptotic effects has been substantiated by an IL-1β/UV-B-driven NF-κB-mediated down-regulation of anti-apoptotic proteins including c-IAP, FLICE-inhibitory protein (FLIP) and TRAF proteins (Poppelmann et al. 2005). Moreover, this decline in the expression of anti-apoptotic proteins is convergent with a release of TNF-α, which now serves as an additional pro-apoptotic stimulus because of the decrease in TRAF proteins (Poppelmann et al. 2005). Based on these findings, the nuclear transcription factor may represent a pivotal molecule in apoptosis, since evidence exists that it works not only in an anti-apoptotic fashion, but also in a pro-apoptotic manner.

For this purpose, the present study explores whether genes involved in the NF-κB and apoptotic pathways represent candidate targets of mechanical forces in primary human PDL fibroblasts (PDL-F). This should contribute to the identification of force-sensing genes in cells of the PDL and may have important implications for the progressive characterisation of cellular effects emanating from the mechanical forces used in orthodontics.

Materials and methods

Cell culture and stretching

This study was approved by the institutional ethic committee of the Medical Faculty, University of Heidelberg (vote no. 148/2003; renewal 30.09.2005). Primary PDL-F were derived from the ligament tissues of periodontally healthy, non-carious human premolar teeth that had been extracted from juvenile donors (age: 12–14 years) for orthodontic reasons with informed consent. Small tissue fragments were established as explant cultures by means of Dulbecco's modified Eagle's medium (PAA, Cölbe, Germany) supplemented with 10% fetal calf serum (FCS; Biochrom, Berlin, Germany), 2 mM L-glutamine (Invitrogen, Karlsruhe, Germany) and antibiotics (kanamycin, 50 mg/ml; Roche, Mannheim, Germany). After nearly reaching confluence, cells were used for stretching experiments between passages 3 and 6. Stretching was carried out according to the method described by Saito et al. (1991). Briefly, following trypsination, $3.5 \times 10^3/cm^2$ PDL cells

were seeded on flexible-bottomed dishes (Greiner Bio-One, Solingen, Germany) covered with coating medium and grown until near-confluence. As an approach to the composition of the ECM environment of PDL-F in vivo, the coating medium consisted of, in addition to 1% bovine serum albumin (Sigma, Munich, Germany), 20 μg/ml native collagen type-I (IBM, Leipzig, Germany) and 10 μg/ml fibronectin (Biomol, Hamburg, Germany), both molecules essentially being found in the ECM of the PDL (Waddington and Embery 2001). The bottom of each dish was stretched by induction of a continuous average stretch of 2.5% (Saito et al. 1991) for periods of 6 h concerning the cDNA and quantitative polymerase chain reaction (q-PCR) experiments, and for 6 h and 12 h in the case of semi-quantitative-PCR (sq-PCR). Irrespective of the *modus operandi*, unstretched cells served as controls. Concerning the forces applied to the PDL-F, the continuous stretch mimicked forces applied during orthodontic tooth movement by using fixed appliances, whereas the chosen time periods, i.e. 6 h and 12 h, reflected the initial stages of therapeutically applied mechanical forces.

RNA extraction and semi-quantitative reverse transcription followed by PCR

Total RNA was isolated from nearly confluent human PDL cells from lumox dishes (Greiner 7Frickenhausen, Germany), after 6 and 12 h periods of strain, by using the PeqGOLD RNA Pure protocol (PEQLAB Biotechnologie, Erlangen, Germany), an optimised guanidine isothiocyanate/phenol method; both the quantity (260 nm) and quality (ratio: 260/280 nm) of the RNA was determined by using a TECAN Genios Plus spectrophotometer (Tecan, Crailsheim, Germany). Reverse transcription (RT) of total RNA (2 μg) was performed by standard protocols with random hexanucleotide priming and RevertAid M-MuLV reverse transcriptase (Fermentas, St. Leon-Rot, Germany) in a total volume of 20 μl. After RT, 1 μl sample was used for PCR. Gene-specific PCRs were performed in a total volume of 30 μl with the gene-specific primers and under the conditions listed in Table 1.

After a general denaturation step at 95°C for 15 min with HotStarTaq DNA Polymerase (Qiagen, Hilden, Germany), denaturing was carried out at 94°C for 1 min for all molecules under study. The annealing temperature ranged from 51°C to 58°C (see Table 1) for 1 min; elongation was performed at 72°C for 1 min. After amplification, 5 μl from each reaction was loaded onto a 2% agarose gel containing ethidium bromide (0.5 μg/ml); the gel was photographed by using a digital camera system (Casio Europe, Norderstedt, Germany). Concomitantly, PCR was performed over 33, 36 and 39 cycles with primers for the housekeeping gene (HKG) calreticulin (Smith and Koch 1989) to allow comparisons of the cDNAs generated from the various cell culture passages and culture conditions. The relative mRNA gene transcription of the genes under study was

Table 1 Primer sequences used for interleukin 1β (IL-1β), nuclear factor kappa B (*NF-κB*), member 6 of the TNF-receptor superfamily (*FAS*), CASP2 and RIPK1 domain-containing adaptor with death domain (*CRADD*), BCL2-antagonist of cell death (*BAD*) and the housekeeping genes (*HKGs*) β-actin and calreticulin in semi-quantitative (*sq-PCR*) and quantitative (*q-PCR*) reverse transcription/polymerase chain reaction (*RT-PCR*)

Molecules	Type of RT-PCR	Primer sequences	Amplicon size (bp)	Annealing temp (°C)
IL-1β	q-PCR	Biomol, Hamburg (PPH00171A)	–	55
	sq-PCR	*Sense:* 5′ ATGGCAGAAGTACCTAAGCTCGC 3′ *Antisense:* 5′ ACACAAATTGCATGGTGAAGTCAGTT 3′	840	58
NF-κB	q-PCR/sq-PCR	*Sense*: 5′ CCGTTATGTATGTGAAGG 3′ *Antisense*: 5′ AGAGTCCAGGATTATAGC 3′	338	53
FAS	q-PCR	Biomol, Hamburg (PPH00141A)	–	55
	sq-PCR	*Sense*: 5′ TCTTTCACTTCGGAGGATTG 3′ *Antisense*: 5′ CACGCAGTCTGGTTCATC 3′	279	55
CRADD	q-PCR	Biomol, Hamburg (PPH00334A)	–	55
	sq-PCR	*Sense*: 5′ TGTGGGCTGAATCCTGAC 3′ *Antisense*: 5′ AACTGAACAATTACAACAATGC 3′	209	51
BAD	q-PCR	*Sense:* 5′ CGAGTGAGCAGGAAGACTCCA 3′ *Antisense:* 5′ AGGAGTCCACAAACTCGTCACT 3′	348	63.3
	sq-PCR	*Sense:* 5′CGAGTGAGCAGGAAGACTCCA 3′ *Antisense:* 5′ AGGAGTCCACAAACTCGTCACT 3′	217	50
HKGs				
β-Actin	q-PCR	Sense: 5′ TTTTTCCAGCAAGTATCCAACC 3′ Antisense: 5′ GGAGTTTTCCAAAGATTTATTGAA 3′	189	55.5
Calreticulin	sq-PCR	Sense: 5′ CTGACCCTGATGCTAAGAA 3′ Antisense: 5′ CTCTTTGCGTTTCTTGTCT 3′	407	51

determined by the ratio of the gene of interest to calreticulin. To generate these data, digital gel images from PCR products and relative densities were determined by using the evaluation software, ImageJ 1.37 h (Wayne Rasband, National Institutes of Health, USA). Each RT-PCR experiment was run three times, based on the primary cell cultures of human PDL cells.

Evaluation was performed by adjusting the density values to the values of the used HKG (calreticulin). The final values were generated by using the mean (±SEM) of three independent experiments. The *P*-values were calculated by the means *t*-test (MedCalc 9.0.1.1, Mariakerke, Belgium), with values of $P<0.01$ being denoted as statistically significant (always compared with the control group).

cDNA array chip hybridisation experiments

We used an apoptosis and NFκ-B pathway GEArray Q Series kit (SuperArray, Bethesda, Md.) according to the manufacturer's instructions. This cDNA expression array contained each of 96 human cDNA fragments from genes associated with the apoptosis or NFκ-B pathway. Briefly, 1–5 μg total RNA prepared by using an RNA extraction kit (RNeasy Mini Kit, Qiagen, Hilden, Germany) was used as a template for cDNA synthesis in a thermal cycler. The annealing mix was prepared with 1 μl GEAprimer Mix, 0.5–5 μg total RNA and RNase-free water to give a final volume of 10 μl. The samples were placed in a thermal cycler at 70°C for 3 min and then cooled down to 37°C for 10 min before addition of the master mix. An RT cocktail was prepared for four samples including GEA buffer (BL, 16 μl), RNase-free water (16 μl), RNase inhibitor (RI, 4 μl) and reverse transcriptase (RE, 4 μl), the nomenclature of the various solutions being as given in the kit. For each array, 10 μl of the RT cocktail were transferred to the 10 μl annealing mixture and incubation was resumed for 25 min at 37°C. Afterwards, the mixture was heated at 85°C for 5 min to hydrolyse the RNA and to inactivate the reverse transcriptase, followed by chilling on ice. Then, the LPR cocktail was prepared for two arrays each (apoptosis and NFκ-B) by the addition of GEA buffer (BL, 36 μl), GEA buffer (AF, 18 μl), biotin-16-dUTP (4 μl, Roche Diagnostics, Mannheim, Germany) and DNA polymerase (LE, 2 μl) to give a final volume of 60 μl. For each array, 30 μl of the LPR cocktail was added to each RT reaction and processed in a thermal cycler under following conditions: 85°C, 5 min; 30 cycles of 85°C for 1 min, 50°C for 1 min, 72°C for 1 min and then finally 72°C for 5 min. RT was stopped by denaturing the sample at 94°C for 2 min and subsequently chilling on ice.

Denatured labelled cDNA probes were added to the arrays and hybridised overnight at 60°C preceding pre-hybridisation with GEAhyb hybridisation solution and heat-denatured sheared salmon sperm DNA. Arrays were then washed and images were obtained via chemiluminescence by using alkaline-phosphatase-conjugated streptavidin and CDP-Star chemiluminescent substrate (Tropix, Bedford, Mass.). After X-ray exposure, the raw image was analysed by using GEArray Analyser software, normalising data to background and the HKG, β-actin (ACTB). For both cDNA arrays, the results from two independent experiments have been exemplified for one array each (Fig. 1).

Real-time q-PCR

RNA extraction and first-strand cDNA synthesis were carried out as described above. cDNA concentrations were determined by fluorometry with a fluorescent dye (Pico-Green, Molecular Probes) and adjusted to 0.5 ng/μl. PCR analysis was performed with the iCycler Real-Time PCR Detection System (BioRad Laboratories, Philadelphia, Pa., USA) according to the manufacturer's instructions. The standard temperature profile included initial denaturation for 3 min at 95°C, followed by 40 cycles of denaturation at 94°C for 40 s, annealing at 55°C to 57°C (primer-dependent) for 30 s and extension at 72°C for 40 s. The sequences of the primers (designed with Beacon Designer 5.0 Software; BioRad Laboratories) and the probes used are listed in Table 1. q-PCR amplification was conducted with a reaction mixture containing 25 μl SYBR green PCR mastermix (iQ SYBR Green Supermix; BioRad Laboratories), 1 μl template cDNA (5 ng) and an appropriate amount of paired primers in a final volume of 50 μl. The results of the q-PCR were analysed as relative expression levels of stretched PDL cells (6 h) in relation to unstretched cells. The relative expression levels of each mRNA were analysed by using a modification of the $\Delta\Delta C_T$ equation, which allows counting for differences in efficiencies ($E=10^{1/slope}$) between the PCRs (Livak and Schmittgen 2001). The data were calculated by using the software Gene Expression Macro provided with the iCycler. Data were obtained from three individual experiments and normalised to the C_T of the HKG, β-actin. The relative expression levels were subjected to the means *t*-test; *P*-values less than 0.01 were considered statistically significant.

Results

Elevation of gene expression of NF-κB-related and apoptosis-related genes in PDL-F identified by cDNA array hybridisation

To contribute to the identification of apoptotic force-sensing genes in primary human PDL-F, we compared the signal intensity of cDNA arrays derived from unstretched

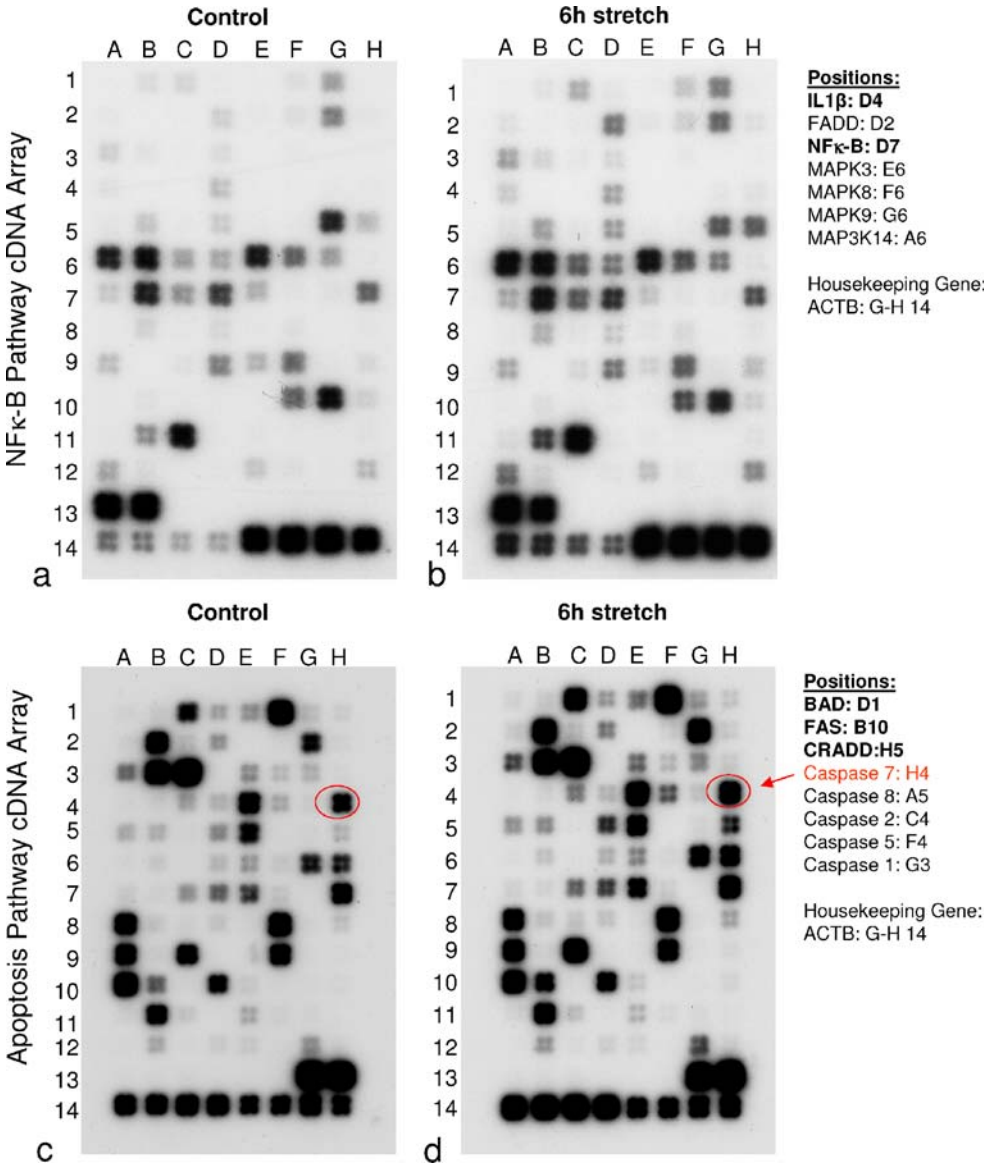

Fig. 1 Representative cDNA micro-array blots illustrating gene expression from stretched (*6h stretch*) and unstretched (*control*) PDL cells. Data were normalised against the housekeeping gene (HKG) β-actin (*ACTB*) and internal background subtraction was applied (GEA-Suite software, Superarray). **a**, **b** NFκ-B pathway cDNA array from total RNA of 6 h stretched and unstretched PDL cells. Examples for modulated NFκ-B-related genes of interest are indicated by their coordinates on the chip. **c**, **d** Apoptosis pathway cDNA array from total RNA of 6 h stretched and unstretched PDL cells. The respective positions of modulated apoptosis-related genes are indicated by their coordinates on the chip (*red circle* position H4 of caspase 7 on the chip). Although not significantly elevated (cut-off level above 1.5 was denoted as significant higher gene expression level compared with the control), caspase 7 revealed 1.4-fold increased gene expression. Genes marked in *bold* have been validated by additional methods including semiquantitative PCR (see Fig. 3) and quantitative PCR (see Fig. 4). Data were obtained from two independent experiments

control PDL-F (Fig. 1a,c) with PDL-F stretched for 6 h (Fig. 1b,d). Since there is growing evidence of an ambivalent role of NF-κB in apoptosis, i.e. mediating anti- and pro-apoptotic signals (Poppelmann et al. 2005), arrays comprising of genes assigned to the NF-κB and apoptosis pathways were employed. By using these arrays, a significant increase (cut-off level 1.5-fold) in gene expression was found for a total of 36 genes, from which 16 rank among the NF-κB and 20 among the apoptosis cDNA array. An overview of these genes, including the numerical value of manifold expression, obtained from the mean of two independent experiments, is given in Table 2 (left: NF-κB-related genes, right: apoptosis-related genes). With respect to NF-κB, an intriguing finding was that the gene expression of this transcription factor was significantly up-regulated in stretched PDL-F. This was exemplified by the representative cDNA microarray blot illustrated in Fig. 1a,b (control versus stretched cells, respectively; coordinate D7).

Figure 2 indicates this up-regulation in more detail by depicting a histogram of the most interesting genes that are significantly increased by stretch. This histogram is based on the means of two individual experiments and reveals a 5.6-fold stretch-dependent NF-κB expression (Fig. 2: blue columns, NF-κB pathway). As reviewed by Pahl (1999), the nuclear transcription factor NF-κB promotes the expression of 150 target genes. On the other hand, the inducers of NF-κB are similar in number and include the pro-inflammatory cytokines TNF-α and IL-1β. Coincident with this description of IL-1β as a potent NF-κB inducer is the finding that, for IL-1β, a stretch-dependent transcriptional elevation can be noted in the PDL-F. This is documented by the cDNA arrays in a comparison of

Table 2 Numerical values of stretch-induced elevated gene expression in periodontal ligament (PDL) fibroblasts as summarised from cDNA chip experiments with an apoptosis and NF-κB pathway cDNA chip. All genes displayed an increase in gene expression, when comparing PDL cells after 6 h stretch versus unstretched control cells. The cut-off level for a significant increase in gene expression was predefined as an increase of at least 1.5-fold. Data were obtained from means of two independent experiments and adjusted to chip-internal controls (housekeeping genes, background subtraction). Genes marked in *bold italics* indicate genes under study

Elevated expression of genes related to NF-κB			Elevated expression of genes related to apoptosis		
Gene	Full name of gene	Value	Gene	Full name of gene	Value
FADD	Fas (TNFRSF6)-associated via death domain	1.97	***BAD***	BCL2-antagonist of cell death	**2.20**
IL1B	Interleukin 1, beta	**3.99**	BAK1	BCL2-antagonist/killer 1	3.14
IRF1	Interferon regulatory factor 1	2.51	BCL10	B-cell CLL/lymphoma 10	3.63
MAP2K4	Mitogen-activated protein kinase kinase 4	4.12	BNIP3	BCL2/adenovirus E1B 19kDa interacting protein 3	2.67
MAP3K1	Mitogen-activated protein kinase kinase kinase 1	2.63	CASP1	Caspase 1, apoptosis-related cysteine protease	3.71
MAP3K14	Mitogen-activated protein kinase kinase kinase 14	12.12	CASP2	Caspase 2, apoptosis-related cysteine protease	4.25
MAP3K2	Mitogen-activated protein kinase kinase kinase 2	3.26	CASP5	Caspase 5, apoptosis-related cysteine protease	7.05
MAPK3	Mitogen-activated protein kinase 3	3.01	CASP8	Caspase 8, apoptosis-related cysteine protease	2.81
MAPK8	Mitogen-activated protein kinase 8	1.60	CASP8AP2	CASP8 associated protein 2	3.69
MYD88	Myeloid differentiation primary response gene (88)	13.71	CHEK1	CHK1 checkpoint homolog	1.89
NFKB1	Nuclear factor of kappa light polypeptide gene enhancer in B-cells 1	**5.61**	***CRADD***	CASP2 and RIPK1 domain containing adaptor with death domain	**8.79**
TLR3	Toll-like receptor 3	8.65	GADD45A	Growth arrest and DNA-damage-inducible, alpha	2.62
TLR4	Toll-like receptor 4	12.52	LTBR	Lymphotoxin beta receptor (TNFR superfamily, member 3)	3.08
TLR5	Toll-like receptor 5	2.32	TNFRSF10A	Tumor necrosis factor receptor superfamily, member 10a	4.61
TLR7	Toll-like receptor 7	6.76	TNFRSF10B	Tumor necrosis factor receptor superfamily, member 10b	1.78
TLR8	Toll-like receptor 8	15.59	TNFRSF1A	Tumor necrosis factor receptor superfamily, member 1A	1.87
			CD40	CD40 antigen (TNF-receptor superfamily member 5)	2.09
			FAS	Fas (TNF-receptor superfamily, member 6)	**3.31**
			TNFRSF8	Tumor necrosis factor receptor superfamily, member 8	1.75
			TNFSF14	Tumor necrosis factor (ligand) superfamily, member 14	1.58

position D4 derived from control (Fig. 1a) and the stretched cells (Fig. 1b) and the elevation level of 3.9-fold expression (Fig. 2: blue columns, NF-κB pathway). Among the plasma-membrane-bound molecules that mediate the activation of NF-κB, the Toll-like receptors occupy an executive position (Kim et al. 2006; Didierlaurent et al. 2006). Concerning these receptors, comparison of the unstretched versus stretched PDL cells indicates a tremendously increased expression of genes encoding for Toll-like receptors 3, 4, 5, 7 and 8 on the NF-κB cDNA array (Table 2, left). This also applies to the myeloid differentiation primary response gene 88 (MYD88) coding for an adapter protein involved in the Toll-like receptor and IL-1 receptor signalling pathway in the innate immune response, thus leading to NF-κB activation (see Table 2, left). Consistent with these findings is the up-regulation of several mitogen-activated protein kinases (MAPKs) and MAPKs-associated kinases (MAPxKx), including MAP3K14. Interestingly, this kinase associated with MAPK3 has been described as being involved in NF-κB induction via cytokines (therefore also termed NF-κB-inducing kinase; Malinin et al. 1997; Yang et al. 2005). Whereas the levels of elevated gene expression range from 1.6-fold up to 4.1-fold for other MAPKs, MAP3K14

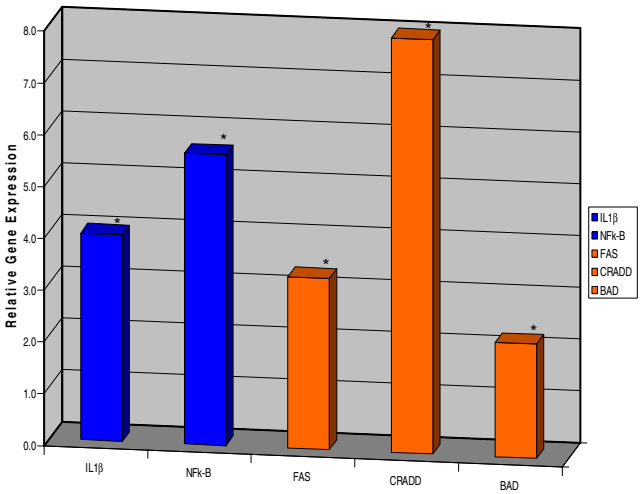

Fig. 2 cDNA micro-array analysis of 6 h stretched and unstretched control PDL cells. The expression levels of apoptosis-related genes IL1β, NFκ-B, FAS, CRADD and BAD after 6 h stretch of PDL cells were plotted as relative gene expression levels compared with unstretched control cells and illustrated as the x-fold higher expression. The data were adjusted to the chip internal housekeeping gene (HKG) β-actin (ACTB); the background was subtracted with the supplied software (GEASuite, Superarray). A cut-off level above 1.5 was designated as being a significantly higher gene expression level compared with the control (*asterisk* significance). Data were obtained from the mean of two independent experiments and adjusted to chip-internal controls (HKG, background subtraction)

displays a 12.1-fold increase upon stretch in PDL-F (Table 2, left, Fig. 1a,b; control versus stretched cells, coordinate A6). Genes exhibiting elevated expression on the apoptosis cDNA array can be attributed to the extrinsic and intrinsic apoptotic pathways, respectively. With respect to intrinsic apoptosis, this holds for the BCL2-antagonists BAK1 and BAD (Table 2, right), the latter also being exemplified in Fig. 1 (compare coordinate D1, Fig. 1c,d, control versus stretched cells, respectively). The 2.2-fold higher expression of BAD in PDL-F after a 6 h mechanical stretch is also depicted in Fig. 2 (orange columns, apoptosis pathway). Concerning extrinsic apoptosis, the CD95 gene encoding for the FAS receptor displays a 3.3-fold stretch-dependent increase (Table 2, right), which is visible not only on the cDNA array (Fig. 1c,d; coordinate B10), but also on the illustration in Fig. 2 (orange columns, apoptosis pathway). Once activated, FAS-induced apoptosis proceeds by the formation of the death-inducing signalling complex, abbreviated DISC (Eramo et al. 2004). One of the pivotal DISC-forming adapter molecules, FADD, shows an approximately 2-fold transcriptional increase (Table 2, left, Fig. 1a,b, coordinate D2). Moreover, molecules comprising the TNF-receptor superfamily (TNFRSF), which can also lead to DISC formation (Ramaswamy et al. 2004) exhibit up-regulated expression levels. This up-regulation is also denoted for TNFRSF 10A, 10B and 1A (Table 2, right). Executioner molecules by which ex- and intrinsic apoptosis pathways are governed include several CASPs. As shown in Fig. 1a,b, CASPs found to be modulated by stretch (control versus PDL cells after a 6-h stretch, respectively) include CASP1 (G3), CASP2 (C4), CASP5 (F4) and CASP8 (A5). Whereas CASP8 (elevation level 2.81, Table 2) is counted among the initiator CASPs (Los et al. 1999) and binds to FADD to complete DISC formation, CASP2 (elevation level 4.2, Table 2) exerts an analogous function in the TNF-R1 signalling complex by binding to its adapter CRADD (Guo et al. 2002). Convergent with a stretch-induced elevation of the aforementioned pro-apoptotic genes, we have also noted such a transcriptional elevation for CRADD (8.79-fold, Table 2), as exemplified by the cDNA array (Fig. 1c,d; coordinate H5) and substantiated by the graphics provided in Fig. 2 (orange columns, apoptosis pathway). cDNAs encoding for molecules that counteract apoptosis remain largely undetectable and are thus not considered here. Such genes include not only the BAD antagonist BCL-2 and some of its dependants, but also members of the TRAF and BIRC/c-IAP proteins, the latter being inhibiting effector CASPs (data not shown).

Confirmation of stretch-dependent transcriptional elevation for selective genes assigned to either the NF-κB or apoptotic pathways by semi-quantitative and quantitative RT-PCR

As summarised in Table 2, 16 NF-κB-related and 20 apoptosis-related genes displaying an elevated expression to mechanical stretch were identified in the present cDNA array analysis. These force-sensing genes could be allocated to well-characterised biological functions. These functions, concerning the NF-κB array, included (1) adapter molecules of death receptors (e.g. FADD), (2) cytokines and regulatory factors (e.g. Il-1β), (3) MAP-kinases/MAPKs and MAPK-associated kinases (e.g. MAP3K14), (4) Toll-like receptors and adapter proteins (e.g. MYD88) and (5) transcription factors (e.g. NF-κB). With respect to the apoptosis array, the identified genes were assigned to functions such as (1) executioners of apoptosis (CASP2), (2) the TNF-receptor superfamily (e.g. CD95/FAS), (3) intrinsic mitochondrial apoptosis (BAD) and (4) adaptor molecules to death domains of death receptors (e.g. CRADD).

To confirm the significantly elevated gene expression indicated in the cDNA data, we selected five genes, two from the NF-κB (IL-1β and NFKB1/NF-κB) and three from the apoptosis array (FAS, CRADD and BAD), as having various levels of differential expression for real-time sq-PCR and q-PCR analysis. As shown in Fig. 3, sq-RT-PCR revealed a stretch-dependent induction or significant elevation in relative mRNA expression in PDL-F. Hereby,

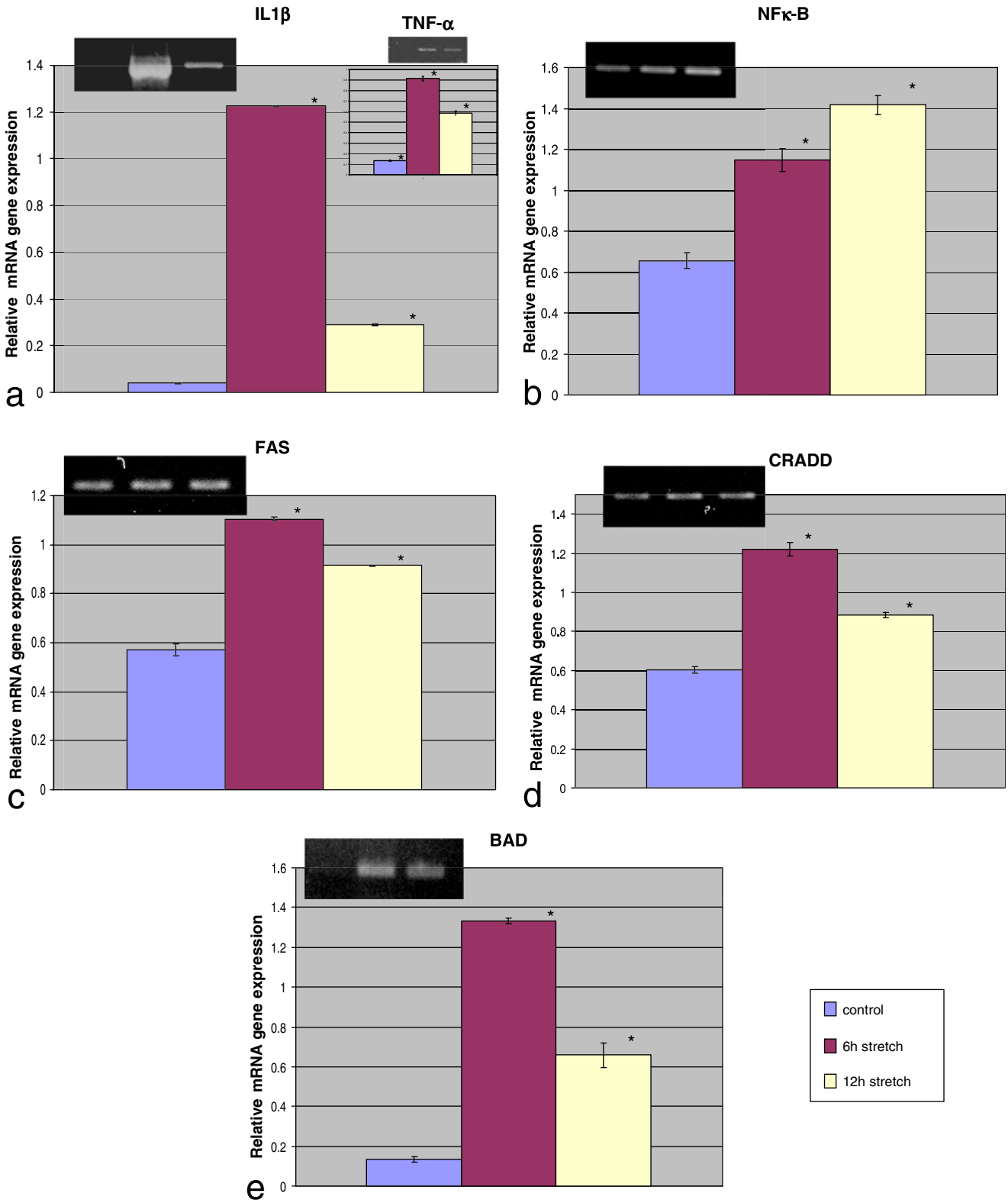

Fig. 3 mRNA expression profiles of apoptosis-related genes in stretched compared with unstretched human PDL cells detected by semi-quantitative RT-PCR. All analysed genes displayed a marked increase or even an induction in relative mRNA gene expression after a 6 h stretch compared with control cells. **a** IL1β (interleukin 1 beta); *inset right*: TNF-α (tumour necrosis factor-α). **b** NFκ-B (nuclear factor kappa B). **c** FAS (TNF-receptor superfamily, member 6). **d** CRADD (CASP2 and RIPK1 domain containing adaptor with death domain). **e** BAD (BCL2-antagonist of cell death). The intensity values of the relevant bands (*insets left*) were generated with quantification software (Image J 5.0) and plotted as the mean values (±SEM) from three individual experiments ($n=3$). Data were adjusted to the HKG, calreticulin (data not shown). *P*-values less than 0.01 were considered statistically significant compared with control: *$P<0.01$

the relative gene expression detected by sq-PCR after 6 h stretch (indicated by the red columns) paralleled the elevated gene expression observed for the selected genes in the respective cDNA arrays. Whereas induced expression could be seen for IL-1β (Fig. 3a) and BAD (Fig. 3e), significantly elevated expression was detected for NFKB1/NF-κB (Fig. 3b), FAS (Fig. 3c) and CRADD (Fig. 3d). To consider a putative time-associated modulation, we analysed the relative expression of the five selected force-sensing target genes at a second time-point, namely at 12 h stretch (yellow bars in Fig. 3). Generally, except for NFKB1 (Fig. 3b), the other selected genes (IL-1β, FAS, CRADD, BAD; Fig. 3a,c–e, respectively) showed lower relative gene expression levels at 12 h of stretch than at 6 h. However, in all cases, the relative expression at 12 h significantly exceeded that of the corresponding controls. These findings suggested a modulation of relative gene expression in response to mechanical forces and time.

Because of the more pronounced differences in relative gene expression recorded for most of the genes at 6 h, q-PCR experiments were carried out at this time-point. The use of a modification of the $\Delta\Delta C_T$ equation revealed that the relative expression levels of stretched PDL cells (6 h) in relation to unstretched cells were basically higher for each mRNA under study (Fig. 4). In detail, the values of manifold expression were 5.8 for IL-1β (Fig. 4, blue column), 1.7 for NFKB1 (pink column), 2.0 for FAS (green column), 2.1 for CRADD (magenta column) and 5.2 for BAD (yellow column). This stretch-induced elevation of relative expression ascertained by q-PCR for all genes agreed with the transcriptional elevation obtained from the cDNA arrays and with the sq-PCR. With regard to the PCR *modi* performed in this study, IL-1β and BAD, which showed induction by stretch in sq-PCR, displayed a more than 5-fold increase in relative gene expression as disclosed by q-PCR.

Discussion

Orthodontic tooth movement is governed by remodelling changes in the cells of the paradental tissues. On the molecular level, these complex changes address, amongst others, the turn-over of proteoglycans, which, in conjunction with collagen type-I, belongs to the main ECM constituents of the PDL and alveolar bone (Waddington and Embery 2001). Further changes include a topographic redistribution and modulation in the activation of components of focal matrix adhesion structures, such as integrins, paxillin and focal adhesion kinase, the last-mentioned being involved in mechanotransduction (Molina et al. 2001).

Recent studies of experimental tooth movement employing animals or cultures of human cells strongly suggest force-driven cell death via apoptosis or an activation of apoptotic pathways (Rana et al. 2001; Hamaya et al. 2002). In human MG-63 osteoblast-like cells, this activation of apoptotic pathways has been substantiated by an activation of CASP3 by means of the CASP8-signalling cascade (Goga et al. 2006). As shown in Table 2, the initiator CASP8 may also represent a candidate target gene of mechanical force in the present study, since we have observed a 2.8-fold elevation in its expression in the human PDL-F, subjected to an average mechanical strain of 2.5%. Further substrates of CASP8, in addition to CASP3, include CASP10, which is situated upstream from CASP3, and also CASP7 and CASP6, which are situated downstream from CASP3. As highlighted in Fig. 1c,d (by coordinate A5), CASP7 displays an expression level of 1.4, which is marginally below the cut off level of 1.5, indicating a significant increase in gene expression. Although marginally lower, the level of 1.4 indicates a slightly increased expression for CASP7, which ranks among the effector CASPs (Los et al. 1999). This slight increase in expression suggests that CASP7 may also represent a possible

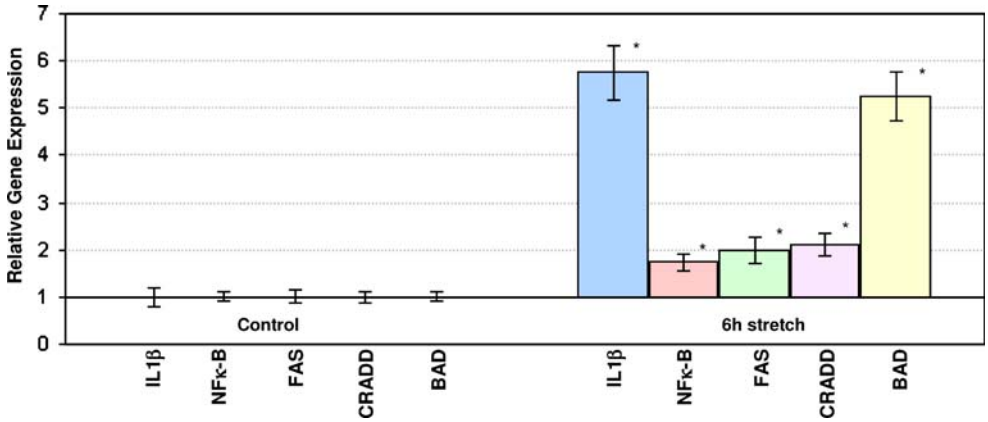

Fig. 4 Differences in relative gene expression level for IL1β (5.8), NFκ-B (1.7), FAS (2.0), CRADD (2.1) and BAD (5.2) between 6 h stretched and unstretched control PDL cells analysed by quantitative RT-PCR. Expression values were normalised to the expression level of β-actin (ACTB) and denoted as mRNA expression relative to control samples. Means (±SEM; $n=3$) were obtained from three individual experiments. *P*-values less than 0.01 were considered statistically significant: $*P<0.01$

substrate for CASP8 in mechanically stretched PDL-F. In the whole of apoptosis originating from the FAS receptor, CASP8 activation precedes the inclusion of its pro-form into the DISC by binding to the adaptor molecule FADD (Wang et al. 1998, 2000). Interestingly, the expression of the genes for the adaptor molecule FADD and the death receptor FAS is significantly addressed by stretch. The transcriptional increase observed for both genes (FADD, 1.97; FAS, 3.31; see Table 2) clearly indicates that they can be allocated to the force-sensing genes. Concerning PDL-F, we can assume that FAS and FADD here potentially allow for the formation of a DISC in response to mechanical forces. Further receptors, capable of inducing apoptosis upon ligand occupancy, belong to the TNF-receptor superfamily and include the TRAIL (TNF-related apoptosis inducing ligand) receptors TRAIL-R1 and -R2 (Merino et al. 2006). Like FAS, the genes encoding for the TRAIL-specific death receptors DR4/TRAIL-R1 and DR5/TRAIL-R2 (see Table 2: TNFRSF10A/DR4, 4.61; TNFRSF10B/DR5, 1.78) also exhibit a stretch-dependent increase in expression. This leads to the assumption that, in PDL cells, death receptors other than FAS may also be involved in a putative force-driven apoptosis. Similar to the FAS-bound DISC, apoptosis evolving from the TNF-receptor requires adaptor molecules, including TRADD (Horssen et al. 2006) and RAIDD. RAIDD, which is also known as CRADD (Guo et al. 2002), facilitates apoptosis via the CASP2-associated signalling cascade. Considering this CASP2-associated pathway, the genes contributing to its initiation, i.e. TNFR-1 (synonym TNFRSF1A; 1.87), CRADD (8.79) and CASP2 (4.25), appear to be up-regulated with regard to their expression in stretch-exposed PDL-F (for all elevation levels, see Table 2). This further strengthens the hypothesis that an onset of apoptosis in response to mechanical forces may not arise exclusively from FAS. Like CASP8, CASP2 is considered an initiator CASP. In this context, it appears noteworthy that the BH3-only protein (also termed BID) provides a substrate for both CASPs, and CASP2 in particular (Bonzon et al. 2006). BID belongs to the BCL-2 family and its cleavage is known to engage the mitochondrial apoptotic pathway (Li et al. 1998; Luo et al. 1998) through direct activation of BAX and possibly BAK (Kuwana et al. 2005). The latter-mentioned molecules, in conjunction with lipids, are assumed to cooperate in the formation of supramolecular openings in the outer mitochondrial membrane (Kuwana et al. 2002). In the PDL-F subjected to mechanical stretch, the genes of both molecules display elevated expression, although the elevation observed for BAX (1.32) is slightly below the level of significance. BAD, a further member of the BCL-2 familiy, is, like BAK, a BCL-2 antagonist, thereby being a pro-apoptotic molecule. With respect to the mitochondrial apoptotic pathway, which also involves BAD (Jiang et al. 2006), this gene has also been found to be significantly elevated (3.2-fold, see Table 2) in its expression during stretch application.

As previously mentioned, activation of the TNF-receptor triggers distinct signalling pathways that may lead to apoptosis (Baud and Karin 2001) and NF-κB activation (Hsu et al. 1995; Krappmann et al. 1996). Although not directly established, the drastic increase of NF-κB expression (5.61, see Table 2, Fig. 2) noted in stretched PDL-F, provides a basis for the possible activation of this nuclear transcription factor. As reviewed by Pahl (1999), potent inducers of NF-κB include the pro-inflammatory cytokines TNF-α and IL-1β, the latter being found as a stretch target in PDL cells as revealed by its 3.99-fold elevation of expression (see Table 2, Fig. 2). The observation of IL-1β being a force-sensing gene in the present study is corroborated by a recent report that has identified IL-1β as a gene related to mechanical stress in PDL cells by employing oligonucleotide-based cDNA arrays (de Araujo et al. 2006). Our own observations obtained from immortalised human gingival keratinocytes have identified the nuclear translocation of NF-κB upon IL-1β stimulation (Steinberg et al. 2006). Therefore, the stretch-induced elevation of IL-β mRNA expression may, even in PDL-F, participate in nuclear NF-κB translocation and subsequent activation. As shown in the inset (right) in Fig. 3a, sq-RT-PCR demonstrates an induced relative expression for TNF-α at both stretching periods under study. This TNF-α induction in stretched PDL-F reveals, on the one hand, that TNF-α may also be a candidate for NF-κB activation and, on the other hand, that TNF-α expression may contribute to the completion of the above-described TNF-receptor/TNF-receptor-mediated apoptosis pathway, because of its potential availability as a TNF-receptor ligand. The possibility of an induction of apoptosis in PDL cells via the TNF pathway, as suggested by the findings of our work, is emphasised by another in vitro study carried out on osteoblasts and PDL cells and showing that apoptosis is triggered by exogenously given TNF-α (Thammasitboon et al. 2006). Inspection of the stretch-responding cDNAs summarised in Table 2 reveals a drastic increase in the expression of genes encoding for several Toll-like receptors. These receptors, like the pro-inflammatory cytokines, are additional inducers of NF-κB and are localised at the plasma membrane of the cells (Kim et al. 2006; Didierlaurent et al. 2006). Interestingly, toxin exposure of macrophages has demonstrated that the activation of Toll-like receptors also induces the gene expression of pro-inflammatory cytokines, including IL-6, Il-1β and TNF-α (Pestka and Zhou 2006), the latter two genes also being addressed by mechanical stretch in our PDL-F. Therefore, in the case of an involvement of Toll-like receptors, PDL-cells may respond to mechanical forces in a dual manner. This duality

may be reflected by either the elevation or induction of expression of genes of the pro-inflammatory cytokines, such as IL-1β and TNF-α, as has also been observed in our study, or the activation of NF-κB. Concerning apoptosis, there is growing evidence that NF-κB operates in an ambivalent fashion by mediating both anti-apoptotic and pro-apoptotic effects. In vitro studies performed on human carcinoma cells have demonstrated that IL-1β-mediated enhancement of UV-B-radiation-induced apoptosis precedes NF-κB activation (Poppelmann et al. 2005); the NF-κB activation in turn causes the repression of anti-apoptotic genes, e.g. members of the TRAF family or c-IAP proteins, respectively. Conversely, a release of TNF-α and activation of the TNF-receptor has been noted. From the down-regulation of anti-apoptotic molecules and the TNF-α release together with TNF-receptor activation, Poppelmann et al. (2005) conclude that NF-κB does not exclusively act in an anti-apoptotic fashion but may also mediate pro-apoptotic effects. Regarding pro-apoptotic effects, NF-κB activation has also been found to up-regulate TRAIL-R2/DR5 upon ligand exposure in epithelial-derived cell lines (Shetty et al. 2005). In addition to these findings, a previously published report of cell lines derived from hepatoma and kidney defines the pro-apoptotic role of NF-κB in mediating FAS/CD95-dependent apoptosis by its transcriptional activation (Kuhnel et al. 2000). With respect to the above-described findings, the implication of an ambiguity of NF-κB in the context of apoptosis should also be taken into consideration for the stretched PDL cells. This consideration is based on the transcriptional increase noted not only for the TNF-α and the TNF-receptor gene, but also for TRAIL receptor 2/DR5 in stretch-exposed PDL-F. Although not analysed in mechanistic terms, stretched PDL-F display a transcriptional elevation for NF-κB and FAS, thereby raising the possibility of an interconnection. On the other hand, for genes antagonising apoptosis, a vice versa situation has been observed, since members of the TRAF and BIRC/c-IAP proteins have not been detected on the cDNA array.

Taken together, this study identifies novel force-sensing genes in stretched PDL-F assigning to the NF-κB and apoptosis pathways, by employing gene-specific cDNA arrays. Many of the genes displaying elevated expression have the ability to induce NF-κB and can be characterised as key players in the initiation and mediation of apoptosis. Therefore, at the initial stage of orthodontic tooth movement, continuous mechanical forces may address not only genes for NF-κB activation and the nuclear transcription factor itself in PDL-F, but also genes for apoptosis arising from the plasma-membrane-bound death receptors and from mitochondria. Transcriptional increase of NF-κB and FAS observed in PDL cells may in addition contribute to the growing evidence of NF-κB occupying an ambiguous role in the apoptotic context, by being either anti- or pro-apoptotic.

References

Araujo RMS de, Oba Y, Moriyama K (2006) Identification of genes related to mechanical stress in human periodontal ligament cells using microarray analysis. J Periodontal Res (Epub ahead of print)

Baud V, Karin M (2001) Signal transduction by tumor necrosis factor and its relatives. Trends Cell Biol 11:372–377

Bolcato-Bellemin AL, Elkaim R, Abehsera A, Fausser JL, Haikel Y, Tenenbaum H (2000) Expression of mRNAs encoding for alpha and beta integrin subunits, MMPs, and TIMPs in stretched human periodontal ligament and gingival fibroblasts. J Dent Res 79:1712–1716

Bonzon C, Bouchier-Hayes L, Pagliari LJ, Green DR, Newmeyer DD (2006) Caspase-2-induced apoptosis requires Bid cleavage: a physiological role for Bid in heat shock-induced death. Mol Biol Cell 17:2150–2157

Chiba M, Mitani H (2004) Cytoskeletal changes and the system of regulation of alkaline phosphatase activity in human periodontal ligament cells induced by mechanical stress. Cell Biochem Funct 22:249–256

Didierlaurent A, Brissoni B, Velin D, Aebi N, Tardivel A, Kaslin E, Sirard JC, Angelov G, Tschopp J, Burns K (2006) Tollip regulates proinflammatory responses to interleukin-1 and lipopolysaccharide. Mol Cell Biol 26:735–742

Eramo A, Sargiacomo M, Ricci-Vitiani L, Todaro M, Stassi G, Messina CG, Parolini I, Lotti F, Sette G, Peschle C, De Maria R (2004) CD95 death-inducing signaling complex formation and internalization occur in lipid rafts of type I and type II cells. Eur J Immunol 34:1930–1940

Goga Y, Chiba M, Shimizu Y, Mitani H (2006) Compressive force induces osteoblast apoptosis via caspase-8. J Dent Res 85:240–244

Guo Y, Srinivasula SM, Druilhe A, Fernandes-Alnemri T, Alnemri ES (2002) Caspase-2 induces apoptosis by releasing proapoptotic proteins from mitochondria. J Biol Chem 277:13430–13437

Hamaya M, Mizoguchi I, Sakakura Y, Yajima T, Abiko Y (2002) Cell death of osteocytes occurs in rat alveolar bone during experimental tooth movement. Calcif Tissue Int 70:117–126

Horssen RV, Rens JA, Schipper D, Eggermont AM, Hagen TL (2006) EMAP-II facilitates TNF-R1 apoptotic signalling in endothelial cells and induces TRADD mobilization. Apoptosis (Epub ahead of print)

Hsu H, Xiong J, Goeddel DV (1995) The TNF receptor 1-associated protein TRADD signals cell death and NF-kappa B activation. Cell 81:495–504

Ingman T, Apajalahti S, Mantyla P, Savolainen P, Sorsa T (2005) Matrix metalloproteinase-1 and -8 in gingival crevicular fluid during orthodontic tooth movement: a pilot study during 1 month of follow-up after fixed appliance activation. Eur J Orthod 27:202–207

Jager A, Zhang D, Kawarizadeh A, Tolba R, Braumann B, Lossdorfer S, Gotz W (2005) Soluble cytokine receptor treatment in experimental orthodontic tooth movement in the rat. Eur J Orthod 27:1–11

Jiang P, Du W, Heese K, Wu M (2006) The bad guy cooperates with good cop p53: Bad is transcriptionally up-regulated by p53 and forms a bad/p53 complex at the mitochondria to induce apoptosis. Mol Cell Biol 26:9071–9082

Kim HA, Cho ML, Choi HY, Yoon CS, Jhun JY, Oh HJ, Kim HY (2006) The catabolic pathway mediated by Toll-like receptors in human osteoarthritic chondrocytes. Arthritis Rheum 54:2152–2163

Krappmann D, Wulczyn FG, Scheidereit C (1996) Different mechanisms control signal-induced degradation and basal turnover of the NF-kappaB inhibitor IkappaB alpha in vivo. EMBO J 15:6716–6726

Krishnan V, Davidovitch Z (2006) Cellular, molecular, and tissue-level reactions to orthodontic force. Am J Orthod Dentofacial Orthop 129:469.e1–e32

Kuhnel F, Zender L, Paul Y, Tietze MK, Trautwein C, Manns M, Kubicka S (2000) NFkappaB mediates apoptosis through transcriptional activation of Fas (CD95) in adenoviral hepatitis. J Biol Chem 275:6421–6427

Kuwana T, Mackey MR, Perkins G, Ellisman MH, Latterich M, Schneiter R, Green DR, Newmeyer DD (2002) Bid, Bax, and lipids cooperate to form supramolecular openings in the outer mitochondrial membrane. Cell 111:331–342

Kuwana T, Bouchier-Hayes L, Chipuk JE, Bonzon C, Sullivan BA, Green DR, Newmeyer DD (2005) BH3 domains of BH3-only proteins differentially regulate Bax-mediated mitochondrial membrane permeabilization both directly and indirectly. Mol Cell 17:525–535

Lee KJ, Park YC, Yu HS, Choi SH, Yoo YJ (2004) Effects of continuous and interrupted orthodontic force on interleukin-1beta and prostaglandin E2 production in gingival crevicular fluid. Am J Orthod Dentofacial Orthop 125:168–177

Li H, Zhu H, Xu CJ, Yuan J (1998) Cleavage of BID by caspase 8 mediates the mitochondrial damage in the Fas pathway of apoptosis. Cell 94:491–501

Liu ZG, Hsu H, Goeddel DV, Karin M (1996) Dissection of TNF receptor 1 effector functions: JNK activation is not linked to apoptosis while NF-kappaB activation prevents cell death. Cell 87:565–576

Livak KJ, Schmittgen TD (2001) Analysis of relative gene expression data using real-time quantitative PCR and the 2(-delta delta C(T)) method. Methods 25:402–408

Los M, Wesselborg S, Schulze-Osthoff K (1999) The role of caspases in development, immunity, and apoptotic signal transduction: lessons from knockout mice. Immunity 10:629–639

Luo X, Budihardjo I, Zou H, Slaughter C, Wang X (1998) Bid, a Bcl2 interacting protein, mediates cytochrome c release from mitochondria in response to activation of cell surface death receptors. Cell 94:481–490

Malinin NL, Boldin MP, Kovalenko AV, Wallach D (1997) MAP3K-related kinase involved in NF-kappaB induction by TNF, CD95 and IL-1. Nature 385:540–544

Meikle MC (2006) The tissue, cellular, and molecular regulation of orthodontic tooth movement: 100 years after Carl Sandstedt. Eur J Orthod 28:221–240

Merino D, Lalaoui N, Morizot A, Schneider P, Solary E, Micheau O (2006) Differential inhibition of TRAIL-mediated DR5-DISC formation by decoy receptors 1 and 2. Mol Cell Biol 26:7046–7055

Molina T, Kabsch K, Alonso A, Kohl A, Komposch G, Tomakidi P (2001) Topographic changes of focal adhesion components and modulation of p125FAK activation in stretched human periodontal ligament fibroblasts. J Dent Res 80:1984–1989

Pahl HL (1999) Activators and target genes of Rel/NF-kappaB transcription factors. Oncogene 18:6853–6866

Pavlin D, Zadro R, Gluhak-Heinrich J (2001) Temporal pattern of stimulation of osteoblast-associated genes during mechanically-induced osteogenesis in vivo: early responses of osteocalcin and type I collagen. Connect Tissue Res 42:135–148

Pestka J, Zhou HR (2006) Toll-like receptor priming sensitizes macrophages to proinflammatory cytokine gene induction by deoxynivalenol and other toxicants. Toxicol Sci 92:445–455

Poppelmann B, Klimmek K, Strozyk E, Voss R, Schwarz T, Kulms D (2005) NF{kappa}B-dependent down-regulation of tumor necrosis factor receptor-associated proteins contributes to interleukin-1-mediated enhancement of ultraviolet B-induced apoptosis. J Biol Chem 280:15635–15643

Ramaswamy M, Efimova EV, Martinez O, Mulherkar NU, Singh SP, Prabhakar BS (2004) IG20 (MADD splice variant-5), a proapoptotic protein, interacts with DR4/DR5 and enhances TRAIL-induced apoptosis by increasing recruitment of FADD and caspase-8 to the DISC. Oncogene 23:6083–6094

Rana MW, Pothisiri V, Killiany DM, Xu XM (2001) Detection of apoptosis during orthodontic tooth movement in rats. Am J Orthod Dentofacial Orthop 119:516–521

Redlich M, Roos H, Reichenberg E, Zaks B, Grosskop A, Bar Kana I, Pitaru S, Palmon A (2004) The effect of centrifugal force on mRNA levels of collagenase, collagen type-I, tissue inhibitors of metalloproteinases and beta-actin in cultured human periodontal ligament fibroblasts. J Periodontal Res 39:27–32

Saito M, Saito S, Ngan PW, Shanfeld J, Davidovitch Z (1991) Interleukin 1 beta and prostaglandin E are involved in the response of periodontal cells to mechanical stress in vivo and in vitro. Am J Orthod Dentofacial Orthop 99:226–240

Sato R, Yamamoto H, Kasai K, Yamauchi M (2002) Distribution pattern of versican, link protein and hyaluronic acid in the rat periodontal ligament during experimental tooth movement. J Periodontal Res 37:15–22

Shetty S, Graham BA, Brown JG, Hu X, Vegh-Yarema N, Harding G, Paul JT, Gibson SB (2005) Transcription factor NF-kappaB differentially regulates death receptor 5 expression involving histone deacetylase 1. Mol Cell Biol 25:5404–5416

Smith MJ, Koch GL (1989) Multiple zones in the sequence of calreticulin (CRP55, calregulin, HACBP), a major calcium binding ER/SR protein. EMBO J 8:3581–3586

Steinberg T, Dannewitz B, Tomakidi P, Hoheisel JD, Mussig E, Kohl A, Nees M (2006) Analysis of interleukin-1beta-modulated mRNA gene transcription in human gingival keratinocytes by epithelia-specific cDNA microarrays. J Periodontal Res 41:426–446

Thammasitboon K, Goldring SR, Boch JA (2006) Role of macrophages in LPS-induced osteoblast and PDL cell apoptosis. Bone 38:845–852

Tuncer BB, Ozmeric N, Tuncer C, Teoman I, Cakilci B, Yucel A, Alpar R, Balos K (2005) Levels of interleukin-8 during tooth movement. Angle Orthod 75:631–636

Waddington RJ, Embery G (2001) Proteoglycans and orthodontic tooth movement. J Orthod 28:281–290

Wang CY, Mayo MW, Korneluk RG, Goeddel DV, Baldwin AS Jr (1998) NF-kappaB antiapoptosis: induction of TRAF1 and TRAF2 and c-IAP1 and c-IAP2 to suppress caspase-8 activation. Science 281:1680–1683

Wang J, Lobito AA, Shen F, Hornung F, Winoto A, Lenardo MJ (2000) Inhibition of Fas-mediated apoptosis by the B cell antigen receptor through c-FLIP. Eur J Immunol 30(1):155–163

Yamaguchi M, Yoshii M, Kasai K (2006) Relationship between substance P and interleukin-1beta in gingival crevicular fluid during orthodontic tooth movement in adults. Eur J Orthod 28:241–246

Yang CH, Murti A, Pfeffer LM (2005) Interferon induces NF-kappa B-inducing kinase/tumor necrosis factor receptor-associated factor-dependent NF-kappa B activation to promote cell survival. J Biol Chem 280:31530–31536